THE JOURNAL OF PHYSICAL CHEMISTRY C

Article

pubs.acs.org/JPCC

Oxygen Activation and Reaction on Pd−Au Bimetallic Surfaces

Wen-Yueh Yu, Liang Zhang, Gregory M. Mullen, Graeme Henkelman, and C. Buddie Mullins*

McKetta Department of Chemical Engineering and Department of Chemistry, Center for Nano and Molecular Science and Technology, Texas Materials Institute, Center for Electrochemistry, and Institute for Computational Engineering and Sciences, University of Texas at Austin, Austin, Texas 78712-0231, United States

Supporting Information

ABSTRACT: Pd−Au bimetallic catalysts have shown promising performance for a number of oxidative reactions. The present study utilizes reactive molecular beam scattering (RMBS), reflection−absorption infrared spectroscopy (RAIRS), temperature-programmed desorption (TPD), and density functional theory (DFT) techniques in an attempt to enhance the fundamental understanding of oxygen activation and reaction with CO on Pd−Au surfaces. Our results reveal that the presence of contiguous Pd sites is crucial for adsorption of oxygen molecules on Pd/Au(111) surfaces at 77 K. Upon heating, oxygen admolecules desorbed molecularly without detectable dissociation in O_2-TPD measurements. CO-RMBS experiments indicate that at lower temperatures (77−150 K) oxygen admolecules were readily displaced by CO due to competitive adsorption. Oxygen admolecules can be thermally activated at higher temperatures (180−250 K) to react with CO to form CO_2. DFT calculations show that the Pd−Au surface containing larger Pd ensembles favors dissociative CO oxidation, whereas associative CO oxidation and O_2 desorption are the two main competing processes for the Pd−Au surface containing small Pd ensembles. An associative CO oxidation pathway was not experimentally observed, which is likely due to facile CO-induced O_2 desorption. These results provide mechanistic insights into the interaction of oxygen with Pd−Au surfaces, which may prove informative for the rational design of Pd−Au catalysts for associated reactions involving O_2 as a reactant.

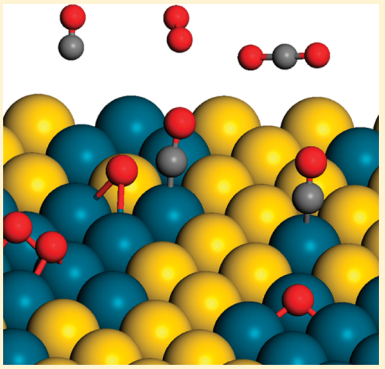

INTRODUCTION

The study of bimetallic catalysts is important in the field of heterogeneous catalysis as bimetallics often exhibit physicochemical properties that are distinctly different from those of the parent metals. These properties provide the potential to design catalysts with enhanced activity, selectivity, and stability.[1,2] As one of the most extensively studied bimetallic systems, Pd−Au catalysts have displayed promising performance in a number of oxidative chemical reactions including CO oxidation,[3,4] acetoxylation of ethylene to vinyl acetate,[5,6] selective oxidation of alcohol to aldehyde,[7−9] and the direct synthesis of hydrogen peroxide from hydrogen and oxygen.[10,11] A molecular-level understanding of how oxygen molecules interact with Pd−Au surfaces (e.g., adsorption, dissociation, and desorption) would be informative for the optimization of Pd−Au catalysts employed for these reactions and other reactions involving oxygen. In model catalyst studies, reactions are normally investigated on well-defined single-crystal surfaces under ultrahigh vacuum (UHV) conditions, which enable the correlation of catalytic properties to surface structures at the molecular level.[1,2,12−16]

Interactions of oxygen with the Pd(111) single-crystal surface have been studied extensively.[17−23] It was reported that oxygen molecularly chemisorbs on the Pd(111) surface at the temperature of 80 K.[19] High-resolution electron energy loss spectroscopy (HREELS)[19,21] showed that chemisorbed oxygen molecules exist in three molecular states that exhibit different vibrational frequencies of O−O stretching due to varying degrees of electron transfer from the surface into the oxygen molecule. At low coverages (dosed by small exposure of molecular oxygen), adsorbed oxygen molecules dissociate into oxygen adatoms at ∼180−200 K,[19−21] which recombine and desorb from the Pd(111) surface at temperatures higher than 600 K in temperature-programmed desorption (TPD) measurements.[18,20] The direct desorption of oxygen admolecules (without dissociation into oxygen adatoms) was observed when molecular oxygen was dosed on the Pd(111) surface at high coverages.[18,20] Three molecular desorption features with peak temperatures of ∼125, 150, and 200 K were observed,[20] which are consistent with the three molecular states characterized in HREELS spectra.[19,21] In contrast to the ease of activation on Pd single-crystal surfaces, it is well-accepted that oxygen molecules do not readily activate (or dissociate) on clean Au single-crystal surfaces.[15,24]

Recently the interaction of oxygen with Pd−Au bimetallic model surfaces has been studied both experimentally[25−27] and theoretically.[28−39] For example, Tysoe and co-workers[25] have investigated the interaction of oxygen with Au/Pd(100) surfaces with various surface compositions using O_2-TPD. Following oxygen exposure at 80 K, direct desorption of oxygen admolecules was observed at 114 and 179 K, and recombinative desorption of oxygen adatoms was detected at ∼750 K during

Received: March 27, 2015
Revised: April 28, 2015
Published: April 29, 2015

DOI: 10.1021/acs.jpcc.5b02970
J. Phys. Chem. C 2015, 119, 11754−11762

heating.[25] The coverage of oxygen adatoms was reported to decrease as the gold coverage was increased.[25] The reaction with CO to form CO_2 is commonly used to probe the reactivity of surface oxygen on Pd−Au model surfaces.[25−28,32,33,35,37−39] By combining reaction kinetics measurements and polarization-modulation infrared reflection spectroscopy (PM-IRAS) characterizations, Gao et al.[26] reported that neither Au nor isolated Pd sites on the AuPd(100) surface are capable of dissociating oxygen molecules. Contiguous Pd sites are required for O_2 dissociation, which in turn accounts for a high CO oxidation activity over the AuPd(110) surface.[26]

In this study, we combine experimental and theoretical methods to investigate the activation of oxygen and its reaction with CO on Pd/Au(111) bimetallic surfaces. The adsorption of oxygen molecules was studied by King−Wells measurements, in which an O_2 beam was impinged onto a variety of Pd/Au(111) surfaces at 77 K. These surfaces were physically characterized employing Auger electron spectroscopy (AES) and reflection−absorption infrared spectroscopy (RAIRS) using CO as a probe molecule. The interactions of oxygen admolecules with Pd/Au(111) surfaces (i.e., desorption and dissociation) were then investigated using O_2-TPD. The energy for O_2 desorption and energy barrier for O_2 dissociation on Pd/Au(111) surfaces with Pd ensembles of various sizes were calculated via DFT methods. CO-RMBS was used to probe the reactivity of oxygen species on Pd/Au(111) surfaces by monitoring CO_2 production. Finally, possible reaction mechanisms (i.e., associative and dissociative pathways) for CO oxidation on Pd/Au(111) surfaces were discussed in terms of the Pd ensemble size using DFT calculations.

EXPERIMENTAL AND COMPUTATIONAL METHODS

UHV Experiments. All experiments in this study were performed in an UHV chamber that has been described in detail previously.[40,41] Briefly, the chamber is equipped with an Auger electron spectrometer (Physical Electronics 10-500), a quadrupole mass spectrometer (Extrel C-50), and a Fourier transform infrared spectrometer (Bruker Tensor 27) combined with a mercury−cadmium−telluride (MCT) detector (Infrared Associates), as well as nozzles and apertures for generating two separate molecular beams.

The Au(111) single-crystal sample is a circular disk (Princeton Scientific, 12 mm in diameter × 2 mm thick) held in place by a Mo wire fitted around a groove cut into the side of the sample. This wire is also used to resistively heat the sample and provide thermal contact between the sample and a liquid nitrogen bath for cooling. The temperature of the sample was measured with a K-type (Alumel−Chromel) thermocouple placed into a small hole in the edge of the disk-shaped sample. The Au(111) surface was periodically cleaned by Ar ion bombardment (2 keV), carried out at room temperature, followed by an anneal to 800 K. The cleanliness of the surface was verified by AES with a beam energy of 3 keV and emission current of 1.5 mA.

Pd−Au bimetallic model surfaces were prepared by depositing ∼2.9 monolayer (ML) of Pd atoms from a homemade thermal evaporator onto the Au(111) surface at 77 K followed by annealing to a specified temperature for 10 min.[42−44] The growth of the Pd overlayer on the Au(111) surface at 77 K is believed to obey a layer-by-layer mechanism, and upon annealing surface Pd atoms can diffuse into the bulk of the Au(111) surface, forming a Pd−Au alloy at the surface.[45] The deposition rate of Pd in this study was calibrated with a quartz crystal microbalance (QCM) controller (Maxtek Inc.) assuming the thickness of 1 ML Pd equals 0.274 nm.

The adsorption of oxygen molecules on Pd−Au surfaces that were annealed to various temperatures (500−675 K) was investigated by King and Wells measurements.[46−49] A neat O_2 molecular beam with a translational energy of ∼0.1 eV was first impinged on the stainless steel inert flag to establish a baseline. The beam was then impinged on the annealed Pd/Au(111) surface at a surface temperature of 77 K. The O_2 QMS signal ($m/z^+ = 32$) was monitored during the King−Wells measurements.

Reflection absorption infrared spectroscopy using CO as a probe molecule (CO-RAIRS) was used to characterize the annealed Pd−Au surfaces. The Pd−Au surface was first heated to 500 K at 1 K/s to desorb any surface contaminants such as CO. After the sample had cooled to 77 K, an IR background scan was taken. Saturation coverage of CO was dosed by a molecular beam of CO with the sample held at 77 K. The IR spectrum of saturated CO adsorbed on the surface was taken at 77 K. All spectra were averaged from 512 scans with a resolution of 4 cm^{-1}.

For O_2-TPD and CO-RMBS experiments, the Pd−Au bimetallic surface was generated by depositing 2.9 ML Pd on the Au(111) surface followed by annealing to 500 K for 10 min. This surface consists of ∼77% Pd and ∼23% Au based on low-energy ion-scattering spectroscopy (LEISS) characterizations.[45] In O_2-TPD measurements, oxygen was dosed by impinging an O_2 beam on the Pd−Au surface at 77 K. The surface was then heated at a rate of 1 K/s, while $m/z^+ = 32$ (O_2) was monitored by QMS. For CO-RMBS experiments, the Pd−Au surface was first saturated with oxygen at 77 K by backfilling the chamber with 1 langmuir (L; 1 L = 1 × 10^{-6} Torr-s) of O_2 through a leak valve. The oxygen-precovered Pd−Au surface was then heated to a specific temperature (77−250 K) prior to CO beam impingement. QMS signals of $m/z^+ = 32$ (O_2), 44 (CO_2), and 28 (CO) were simultaneously monitored during CO-RMBS experiments.

DFT Calculations. All DFT calculations were performed with the Vienna ab initio simulation package.[50−53] The interaction between the ionic core and the valence electrons was described by the project augmented wave method,[54] and the valence electrons were described with a plane-wave basis up to an energy cutoff of 300 eV.[55,56] The energy cutoff was increased to 400 eV to test for convergence, and the O_2 dissociation barrier on Au was found to vary by less than 0.005 eV. The exchange correlation contribution to the total energy functional was determined using the Perdew−Burke−Ernzerhof (PBE) generalized gradient approximation functional.[57] The location and energy of the transition states were calculated with the climbing-image nudged elastic band method.[58,59] The gold surface was modeled as a four-layer 4 × 4 Au(111) slab with the bottom two layers fixed and 10 Å of vacuum. The Pd-decorated Au(111) surfaces in this study are modeled by replacing Au atoms on the top layer of the Au(111) slab with various Pd ensembles, as illustrated in Figure S1 (Supporting Information). The Brillouin zone was sampled using a 3 × 3 × 1 Monkhorst−Pack k-point mesh.[60] The convergence criteria for the electronic structure and the atomic geometry were 10^{-5} eV and 0.01 eV/Å, respectively. The binding energies of O_2 and CO on the surface are referenced to the gas-phase O_2 and CO molecules, respectively.

DOI: 10.1021/acs.jpcc.5b02970
J. Phys. Chem. C 2015, 119, 11754−11762

RESULTS AND DISCUSSION

Adsorption of Oxygen on Pd–Au Surfaces. In this study, the adsorption of oxygen molecules on Pd–Au surfaces was investigated by King–Wells measurements. Figure 1 shows

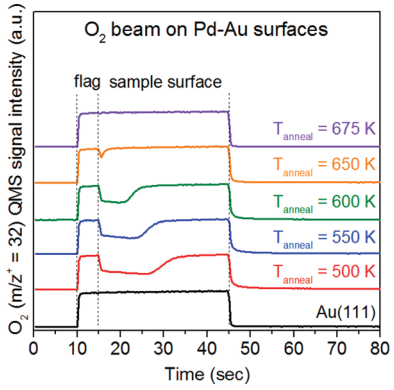

Figure 1. King–Wells measurements of an O_2 beam impinging on Au(111) and annealed 2.9 ML Pd/Au(111) surfaces at a surface temperature of 77 K.

the O_2 QMS signal during a series of King–Wells measurements in which an O_2 beam was impinged onto the 2.9 ML Pd/Au(111) surface that was previously annealed to various temperatures (i.e., 500–675 K). The O_2 molecular beam was first impinged onto the inert flag that was held in front of the sample surface for 5 s (from 10 to 15 s) to establish a baseline signal (all O_2 molecules scattering from the inert flag). After removing the inert flag, the beam was impinged onto the Pd–Au surface that was held at 77 K for 30 s (from 15 to 45 s). The measurement was also conducted on the clean (Pd-free) Au(111) surface and is included for comparison.

When the O_2 beam was impinged on the inert flag, a constant O_2 QMS signal was detected due to scattering of the beam with negligible adsorption on the sample. After the removal of the inert flag, a constant O_2 QMS signal was observed from the clean Au(111) surface, signifying no oxygen adsorption (or uptake) occurred on the clean Au(111) surface.

For the Pd/Au(111) surface annealed to 500 K, the intensity of the O_2 QMS signal was initially lower than that observed for impingement onto the inert flag due to the adsorption of oxygen on the surface. Since no oxygen uptake was observed on the Au(111) surface, it is proposed that the adsorption sites for oxygen on the annealed Pd/Au(111) surface consist of Pd surface atoms. It has been reported that with exposure to oxygen molecules at 100 K oxygen adsorbs molecularly on the Pd(111) surface, and the dissociation of oxygen admolecules occurs at temperatures of ~180–200 K.[20] Accordingly, the oxygen adsorption on the Pd–Au surface observed here is likely molecular adsorption without dissociation. The initial sticking probability of oxygen is ~0.43 for the Pd/Au(111) surface annealed at 500 K. The sticking probability eventually decreases to zero (where the intensity of the O_2 QMS signal from the sample surface became nearly identical with that from the inert flag) as adsorbed oxygen saturated the Pd–Au surface.

When the Pd/Au(111) surface was progressively annealed to higher temperatures (550–675 K), the time to saturate the surface with oxygen molecules gradually reduced, indicative of less oxygen uptake since the flux of the O_2 beam was kept constant for all of these measurements. The uptake of oxygen on each surface during the King–Wells measurements is proportional to the magnitude of integral of the intensity of the O_2 QMS signal from the sample surface using the intensity of the O_2 QMS signal from the inert flag as a baseline (Figure S2, Supporting Information). Relative to the Pd/Au(111) surface annealed at 500 K, the oxygen uptake for Pd/Au(111) surfaces annealed to 550, 600, and 650 K reduced to ~75%, 49%, and 2%, respectively. The oxygen uptake was negligible on the Pd/Au(111) surface that was annealed at 675 K.

The oxygen uptake on the Pd–Au surface is correlated with the concentration of surface Pd atoms. We characterized the relative surface compositions for annealed Pd/Au(111) surfaces by AES. Figure S3 (Supporting Information) shows the AES spectra of as-prepared and annealed 2.9 ML Pd/Au(111) surfaces. As the annealing temperature was increased, the Pd AES signal intensity was attenuated, and the Au AES signal intensity was enhanced, which has been previously observed by Koel and co-workers.[45] This effect is attributed to diffusion of surface Pd atoms into the subsurface of the Au(111) single-crystal sample during the annealing process.[45] The oxygen uptake during King–Wells measurements as a function of the Pd/Au AES signal intensity ratio of each annealed surface is illustrated in Figure 2.

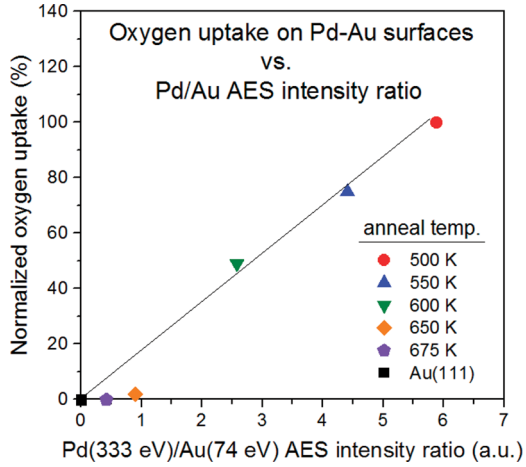

Figure 2. Oxygen uptake during King–Wells measurements on annealed 2.9 ML Pd/Au(111) bimetallic surfaces versus Pd (333 eV)/Au (74 eV) AES intensity ratio.

The oxygen uptake is linearly proportional to the Pd/Au AES signal intensity ratio for all surfaces except those that were annealed at 650 and 675 K. This deviation suggests that other surface properties (e.g., arrangement of Pd and Au surface atoms) may also influence the oxygen uptake on the Pd–Au surface, and oxygen uptake may not simply be a function of the concentration of Pd atoms on the Pd/Au(111) surface.

The annealed Pd/Au(111) surfaces were further characterized by RAIRS using CO as a probe molecule (CO-RAIRS). CO-RAIRS has been extensively employed to characterize the surface properties and structures of the Pd–Au model surface.[6,26,42,61–63] The type of adsorption site occupied by CO (e.g., atop sites, 2-fold or 3-fold bridge sites) can be inferred by the intramolecular CO stretch frequency (ν_{CO}) as a result of varying degrees of π-antibonding back-donation from the surface electrons.[64] Figure 3 shows the RAIRS spectra for saturated CO adsorbed on the clean Au(111) and annealed 2.9 ML Pd/Au(111) surfaces at 77 K.

DOI: 10.1021/acs.jpcc.5b02970
J. Phys. Chem. C 2015, 119, 11754–11762

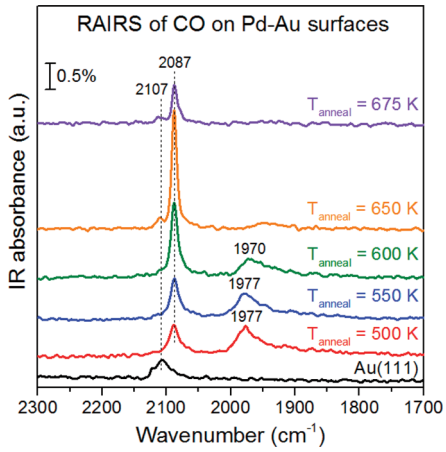

Figure 3. RAIRS spectra of saturated CO on Au(111) and annealed 2.9 ML Pd/Au(111) bimetallic surfaces taken at a surface temperature of 77 K.

For the clean Au(111) surface, only one vibrational band at ~2107 cm^{-1} was observed, which is associated with CO bound to atop Au sites.[26,61−63,65] The Pd/Au(111) surface annealed at 500 K displayed two IR features at ~2087 and ~1977 cm^{-1}, which have been assigned to atop CO on isolated Pd sites (or Pd monomer) and bridged CO on contiguous Pd sites, respectively.[26,61−63] Increasing the annealing temperature resulted in the attenuation of the IR signal associated with bridged CO on contiguous Pd sites (ν_{CO} = ~1977 cm^{-1}) and intensification of the signal associated with CO atop on isolated Pd sites (ν_{CO} = ~2087 cm^{-1}). The IR band due to bridged CO on contiguous Pd sites became relatively small for the Pd/Au(111) surfaces annealed at 650 K and disappeared when annealed at 675 K. Considering the CO-RAIRS spectra (Figure 3) and oxygen uptake (Figure 2), it suggests that the presence of contiguous Pd sites on the Pd−Au surface is crucial for adsorption of oxygen molecules.

These experimental observations are conceptually consistent with our DFT calculations of oxygen adsorption. The binding energy of an oxygen molecule as a function of Pd ensemble size on Pd/Au(111) surfaces is presented in Figure S4 (Supporting Information). As shown in the inset of Figure S4 (Supporting Information), molecular oxygen binds on the fcc hollow site aligned in a top-hollow-bridge (t-h-b) geometry on these surfaces, except for the Pd_2−Au(111) surface, where the oxygen molecule bridges on two Pd atoms. The calculated binding energy for the oxygen molecule on the Au(111) surface is 0.34 eV. With the presence of the Pd monomer, the binding energy decreases to 0.11 eV on the Pd_1−Au(111) surface. These positive values of binding energy indicate that the adsorption of an oxygen molecule is energetically unfavorable on the clean Au(111) and Pd_1−Au(111) surfaces. The binding energy of the oxygen molecule reduces to the negative value of −0.17 eV on the Au(111) surface with a Pd dimer (i.e., Pd_2−Au(111) surface), which supports our experimental observation of the importance of contiguous Pd sites for adsorption of oxygen molecules on the Pd−Au surface. These results are also consistent with previous DFT reports, in which the effects of Pd ensembles (i.e., monomer, dimer, and trimer) on the adsorption oxygen molecule were investigated using 1 ML Au/Pd(111)[29] and Au(111) surfaces[35] as substrates. The binding energy of the oxygen molecule on the Pd/Au(111) surface gradually decreases as the Pd ensemble size increases. For the Au(111) surfaces fully covered by 1 ML of Pd overlayer, the calculated binding energy of the oxygen molecule is −0.83 eV, indicating that the oxygen molecule binds more strongly to this surface than to other Pd/Au(111) surfaces.

Desorption of Oxygen from Pd−Au Surfaces. The interaction of oxygen with the Pd−Au surface was investigated via O_2-TPD as shown in Figure 4. The Pd−Au surface was

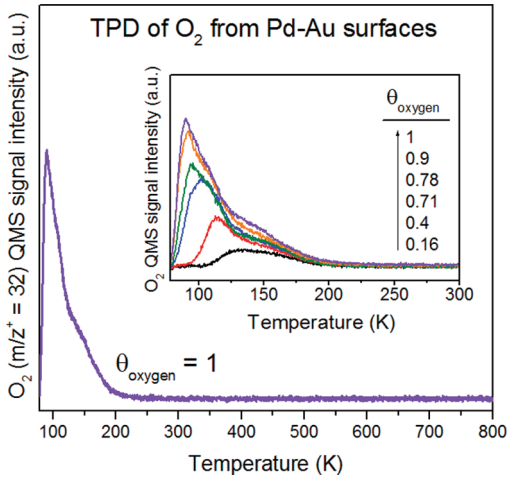

Figure 4. TPD of saturated O_2 from the Pd/Au(111) bimetallic surface. Inset shows the TPD of various coverages of O_2 from the same surface. The heating rate was 1 K/s.

generated by depositing 2.9 ML Pd onto the Au(111) surface at 77 K followed by annealing at 500 K. Dosing of O_2 was achieved by impinging a molecular beam of O_2 onto the surface at 77 K prior to heating.

O_2-TPD has been extensively studied on the Pd(111) surface.[17,18,20,21] According to the desorption temperature, two types of oxygen desorption processes have been identified from the Pd(111) surface:[20] associative desorption (or recombinative desorption of oxygen adatoms; peak temperature at ~800 K) and molecular desorption (or direct desorption of oxygen admolecules; peak temperatures at ~200, 150, and 125 K). In Figure 4, the oxygen desorption peak ended at ~220 K, and no other feature was observed during heating to 800 K. These results suggest that oxygen admolecules desorb molecularly from the Pd−Au surface without detectable dissociation into oxygen adatoms. It is noted that the Pd/Au(111) surface that was generated by annealing at 500 K undergoes significant changes when the temperature is heated to above 500 K (as shown in AES (Figure S3, Supporting Information) and CO-RAIRS (Figure 3) characterizations), which increases the difficulty of investigating the phenomena for recombinative desorption of oxygen adatoms during heating. Nevertheless, it is clear that the surface concentration of oxygen adatoms from dissociation of oxygen molecules (if any) is not sufficient to detect via O_2-TPD. The inset in Figure 4 shows desorption of oxygen molecules with various coverages from the Pd−Au surface. In these TPD measurements, various coverages of oxygen were dosed onto the same Pd−Au surface at 77 K followed by heating to 500 K. To more clearly visualize desorption peaks, the obtained spectra were plotted within the temperature range between 77 and 300 K (no oxygen desorption was observed when the temperature was higher than 300 K) as shown in the inset of Figure 4. In contrast with the sharp features in molecular oxygen desorption observed

DOI: 10.1021/acs.jpcc.5b02970
J. Phys. Chem. C 2015, 119, 11754−11762

from the Pd(111) surface,[20] the desorption peaks for oxygen molecules from the Pd−Au surface are relatively broad, which is likely due to the relatively high degree of heterogeneity of the annealed Pd/Au(111) surface in comparison to that of the Pd(111) surface.

The competition between desorption and dissociation of the molecular oxygen on Pd−Au surfaces upon heating was also explored by DFT calculations. Figure 5 represents the energy for desorption and energy barrier for dissociation of an oxygen molecule on Pd/Au(111) surfaces as a function of Pd ensemble size. The corresponding potential energy diagram is shown in Figure S5 (Supporting Information). It is noted that the energy for desorption of the oxygen admolecule is essentially the negative value of the binding energy shown in Figure S4 (Supporting Information).

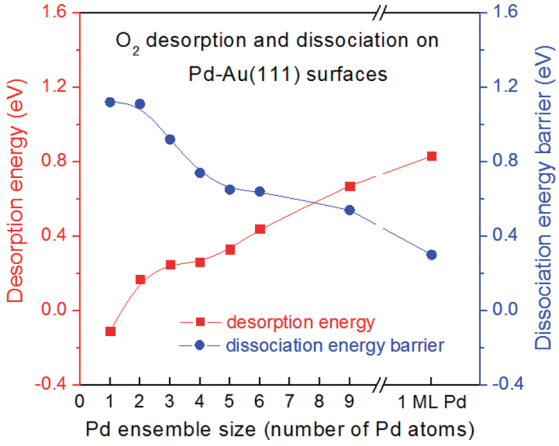

Figure 5. Energy for desorption and energy barrier for dissociation of an oxygen molecule adsorbed on Pd/Au(111) surfaces as determined by DFT calculations.

As shown in Figure 5, the energy for desorption of an oxygen admolecule (i.e., $O_{2(ad)} \rightarrow O_{2(g)}$) gradually increases from 0.17 to 0.44 eV as the Pd ensemble on the Au(111) surface changes from a dimer to a hexamer. On the other hand, the energy barrier for dissociation of an oxygen admolecule (i.e., $O_{2(ad)} \rightarrow 2O_{(ad)}$) decreases from 1.11 to 0.64 eV under the same conditions. It is noted that the energy for desorption is smaller than the energy barrier for dissociation on each of these Pd/Au(111) surfaces. Furthermore, it has been reported that the desorption prefactor (ν_{des}) is usually significantly larger than the dissociation prefactor (ν_{diss}) for a molecular adsorbate ($\nu_{diss} = \sim 10^{-3}\ \nu_{des}$).[66] Accordingly, desorption of O_2 is favored over its dissociation on these Pd/Au(111) surfaces. In other words, upon heating, the oxygen admolecule would prefer to desorb from the surface at the temperature below its dissociation temperature. These results are in good agreement with our O_2-TPD observations (Figure 4), in which molecular desorption of oxygen was observed, but the recombinative desorption of atomic oxygen that comes from dissociation was undetectable. As shown in Figure 5, the dissociation of an oxygen admolecule becomes energetically favorable over desorption when larger Pd ensembles (e.g., consisting of nine Pd atoms) are present on the Au(111) surface. For the Au(111) surface covered by 1 ML of Pd (i.e., the Pd_{1ML}/Au(111) surface), the calculated energy barrier for dissociation of an oxygen admolecule (0.3 eV) is much lower than the energy for desorption of an oxygen admolecule (0.83 eV). This is consistent with the observation that low coverages of oxygen admolecules can completely dissociate into oxygen adatoms on the Pd(111) surface.[20]

Reaction of Oxygen and CO on Pd−Au Surfaces. The reaction with CO to form CO_2 has been used to experimentally probe the reactivity of surface oxygen on Pd−Au model surfaces.[25−27] In this study, the reactivity of molecular oxygen adsorbed on the Pd/Au(111) surface upon heating was assessed by CO-RMBS via monitoring CO_2 production. CO-RMBS experiments were conducted by impinging a molecular beam of CO onto the inert flag for 5 s (from 15 to 20 s) and then onto the molecular oxygen-precovered Pd−Au surface for 60 s (from 20 to 80 s) as shown in Figure 6. For these measurements, the Pd−Au surface (generated by depositing 2.9 ML Pd onto the Au(111) surface at 77 K followed by annealing at 500 K) was presaturated with molecular oxygen at 77 K and then heated to a specific temperature (77−250 K) prior to CO beam impingement. The measured O_2 and CO_2 QMS signals are depicted in Figures 6a and 6b, respectively.

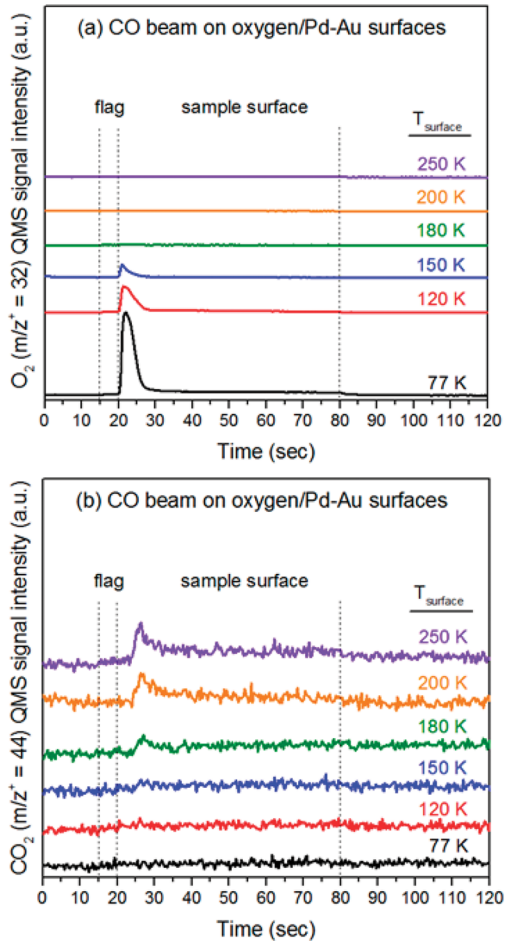

Figure 6. (a) O_2 ($m/z^+ = 32$) and (b) CO_2 ($m/z^+ = 44$) QMS signals during CO-RMBS on the oxygen-presaturated Pd/Au(111) bimetallic surface at various surface temperatures.

As expected, neither O_2 nor CO_2 QMS signals were detected when the CO beam was impinged onto the inert flag. When the CO beam struck the oxygen-precovered Pd−Au surface at 77 K, a peak in the O_2 QMS signal emerged (Figure 6a), indicating that impingement of CO onto the surface caused evolution of O_2. This O_2 evolution is likely due to the competitive adsorption of CO on the surface sites, which displaces the

DOI: 10.1021/acs.jpcc.5b02970
J. Phys. Chem. C 2015, 119, 11754−11762

preadsorbed O_2 into the gas phase. Since no measurable O_2 adsorption was detected when an O_2 beam struck the CO-presaturated Pd–Au surface at 77 K (Figure S6, Supporting Information), we speculate that the adsorption strength of CO on the surface is much stronger than that of O_2. This suggestion is also supported by DFT calculations in which the binding of CO (Figure S7, Supporting Information) to Pd/Au(111) surfaces is found to be stronger relative to that of O_2 (Figure S4, Supporting Information). The oxygen evolution decreased in intensity when the Pd–Au surface was preheated to 120 K, which is likely due to desorption of O_2 during heating (Figure 4) before CO beam impingement. The intensity of oxygen evolution decreased further as the surface was preheated and held at higher temperatures (180–250 K).

As shown in Figure 6b, no CO_2 signal was detected when the CO beam was impinged onto the oxygen-precovered Pd–Au surface held at temperatures ranging from 77 to 150 K. These results show that the surface oxygen species is inactive to react with CO to form CO_2 within this temperature range (77–150 K). A small peak in CO_2 production was observed when the CO beam struck the oxygen-precovered Pd–Au surface at 180 K, suggestive of the thermal activation of adsorbed oxygen molecules. It is noted that the CO_2 peak emerged at ~24 s, which is ~4 s after CO beam impingement which began at 20 s. This is likely due to the site blocking from oxygen and hydrogen impurities (from adsorption of background gas that is intrinsically present in our UHV chamber)[42] on the Pd–Au surface. Figure S8 (Supporting Information) shows the QMS signals of O_2, CO_2, H_2, and CO during a CO-RMBS experiment at 180 K. The emergence of a CO_2 production peak was observed after the evolution of O_2 and H_2 that were induced by CO beam impingement. The phenomena of CO-induced recombinative desorption of H adatoms from the Pd/Au(111) surface have been observed previously.[43]

The CO_2 production peak became more significant when the surface was heated to higher temperatures (200 and 250 K) prior to CO beam impingement. As shown in Figure 4, the process for molecular desorption of adsorbed oxygen ended at a temperature of ~220 K. Accordingly, the CO_2 production from the Pd–Au surface observed at 250 K is likely due to the reaction of CO with oxygen adatoms rather than oxygen admolecules. This observation suggests that dissociation of oxygen admolecules could occur on the Pd–Au surface during heating (the amount of oxygen that reacted with CO above 200 K is estimated as ~0.3% of saturation oxygen coverage), which was undetected in the O_2-TPD measurements in Figure 4. It is noted that oxygen admolecules dissociate into oxygen adatoms on the Pd(111) surface at ~180–200 K,[19−21] which is coincident with the temperature range in which we observed CO_2 production from the reaction of CO with oxygen species on the Pd–Au surface in CO-RMBS experiments (Figure 6b).

DFT calculations were performed to examine the influence of the Pd ensemble size on the reaction mechanism of CO oxidation on Pd–Au surfaces. In this study, we consider two possible Langmuir–Hinshelwood mechanisms, i.e., dissociative and associative mechanisms, as shown in Scheme 1.[33]

The dissociative and associative mechanisms are different from each other in regards to their initial step. For the dissociative mechanism, the O_2 admolecule dissociates into O adatoms as the first step (step A). In the associative mechanism, the first step is the bimolecular reaction between the O_2 admolecule and adsorbed CO to form adsorbed CO_2 and an O adatom (step C). The dissociative and associative mechanisms result in the same overall reaction as the second step (step B); i.e., the O adatom reacts with adsorbed CO to form adsorbed CO_2.[33]

Scheme 1. Potential Dissociative and Associative Mechanisms for the Reaction of Oxygen with CO to Form CO_2[33]

Dissociative mechanism

$O_{2(ad)} \rightarrow 2\ O_{(ad)}$ (A)

$O_{(ad)} + CO_{(ad)} \rightarrow CO_{2(ad)}$ (B)

Associative mechanism

$O_{2(ad)} + CO_{(ad)} \rightarrow CO_{2(ad)} + O_{(ad)}$ (C)

$O_{(ad)} + CO_{(ad)} \rightarrow CO_{2(ad)}$ (B)

Figure 7 shows the calculated energy barriers for each step in the dissociative and associative CO oxidation on Pd/Au(111) surfaces. The corresponding reaction enthalpies are summarized in Table S1 (Supporting Information). It is noted that the Pd–Au surfaces with a Pd ensemble size of less than four atoms are excluded due to the lack of a capacity for CO and O_2 coadsorption. The initial, transition, and final state configurations on each surface are similar; accordingly, only those on the Pd_6–Au(111) surface are illustrated in Figure S9 (Supporting Information) as an example.

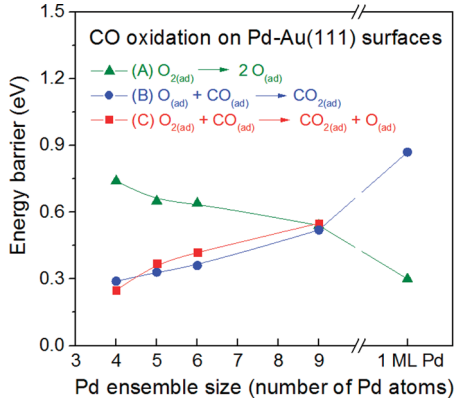

Figure 7. Energy barriers for dissociative and associative CO oxidation on Pd/Au(111) surfaces as determined by DFT calculations.

On the Pd_4–Au(111) surface, the energy barriers for $O_{2(ad)} \rightarrow 2O_{(ad)}$ (step A), $O_{(ad)} + CO_{(ad)} \rightarrow CO_{2(ad)}$ (step B), and $O_{2(ad)} + CO_{(ad)} \rightarrow CO_{2(ad)} + O_{(ad)}$ (step C) are 0.74, 0.29, and 0.25 eV, respectively. These results suggest that associative CO oxidation is favorable on this surface, whereas dissociative CO oxidation is inhibited by a higher energy barrier for dissociating the O_2 admolecule. It is worth mentioning that the energy for O_2 desorption on the Pd_4–Au(111) surface is 0.26 eV (Figure 5), which is comparable to the reaction barriers for $O_{(ad)} + CO_{(ad)} \rightarrow CO_{2(ad)}$ (step B) and $O_{2(ad)} + CO_{(ad)} \rightarrow CO_{2(ad)} + O_{(ad)}$ (step C).

As the Pd ensemble size increases, the energy barrier for O_2 dissociation (step A) reduces, while energy barriers for $O_{(ad)} + CO_{(ad)} \rightarrow CO_{2(ad)}$ (step B) and $O_{2(ad)} + CO_{(ad)} \rightarrow CO_{2(ad)} + O_{(ad)}$ (step C) both increase. These energy barriers become comparable on the Pd_9–Au(111) surface, which suggests that CO oxidation could proceed via both associative and dissociative pathways on this surface. As mentioned earlier, the dominant oxygen species on the Pd_{1ML}–Au(111) surface is the O adatom rather than the O_2 admolecule due to a lower energy barrier for O_2 dissociation. Accordingly, dissociative CO

DOI: 10.1021/acs.jpcc.5b02970
J. Phys. Chem. C 2015, 119, 11754–11762

oxidation is favorable on the Pd_{1ML}–Au(111) surface, which is consistent with the experimental observations from the Pd(111) surface.[67−71]

On the basis of these DFT calculations, a generalization regarding the effect of Pd ensemble size on oxygen activation and reaction with CO was derived as follows: for the Pd–Au surface containing small Pd ensembles, O_2 desorption and associative CO oxidation are the two major competing processes, whereas the pathway for dissociative CO oxidation is limited by a high energy barrier for O_2 dissociation. On the Pd–Au surface with bigger Pd ensembles, the oxygen admolecule dissociates readily and, in turn, promotes CO_2 formation via the dissociative CO oxidation pathway. It is well-accepted that CO oxidation occurs on the Pd(111) surface via a dissociative pathway,[67−71] in which chemisorbed CO reacts with dissociatively adsorbed oxygen to form CO_2. DFT calculations in this study and previous reports[32,35] suggest that CO oxidation could also occur through an associative mechanism on the Pd–Au surface containing small Pd ensembles. Nevertheless, it is noted that an associative pathway was not experimentally supported in this study (Figure 6b), in which no CO_2 production was detected when the CO beam was impinged onto the molecular oxygen-precovered Pd–Au surface at and below 150 K. This absence of CO_2 production can be explained by the facile CO-induced displacement of O_2 (Figure 6a) due to significantly higher binding energies of CO relative to those of O_2 (Figures S4 and S7, Supporting Information), which inhibits CO oxidation from proceeding via associative mechanism.

CONCLUSION

A model catalyst study combining UHV experiments and DFT calculations was performed to investigate the activation and reaction of oxygen molecules on the Pd–Au surface. Results based on O_2 King–Wells, CO-RAIRS, and DFT show that the presence of contiguous Pd sites is essential for adsorption of oxygen molecules on the Pd–Au surface. Upon heating, the adsorbed oxygen molecules molecularly desorbed from the Pd–Au surface (<220 K) without detectable dissociation (signified by a lack of recombinative desorption of oxygen atoms) in O_2-TPD experiments. DFT calculations show that as the Pd ensemble size increases on the Pd/Au(111) surface the energy for O_2 desorption increases, and the energy barrier for O_2 dissociation decreases. Oxygen molecules adsorbed on the Pd/Au(111) surface were readily displaced by CO at lower temperatures (77–150 K) due to competitive adsorption on surface sites. The adsorbed oxygen molecule can be thermally activated at higher temperatures (180–250 K) to react with CO to form CO_2. On the basis of DFT calculations, dissociative CO oxidation is favorable on the Pd–Au surface containing larger Pd ensembles; for the Pd–Au surface containing small Pd ensembles, associative CO oxidation and O_2 desorption are the two competing processes that are both favored over dissociative CO oxidation. In this study, an associative CO oxidation mechanism was not experimentally observed on the Pd–Au surface, which could be attributed to the fact that weakly bound O_2 desorbs readily by CO displacement at low temperatures. We hope the findings in this study will assist in the future design of Pd–Au bimetallic catalysts and their applications to associated reactions.

ASSOCIATED CONTENT

Supporting Information

Additional information regarding Pd/Au(111) surfaces for DFT calculations, O_2 King–Wells measurements for annealed Pd/Au(111) surfaces, AES characterizations for as-deposited and annealed Pd/Au(111) surfaces, binding energies for O_2 on Pd/Au(111) surfaces, potential energy diagram for O_2 desorption and dissociation on Pd/Au(111) surfaces, O_2 King–Wells measurement for the CO-presaturated Pd/Au(111) surface, binding energies for CO on Pd/Au(111) surfaces, CO-RMBS on oxygen-precovered Pd/Au(111) surface, dissociative and associative CO oxidation on Pd/Au(111) surfaces; illustration of Pd/Au(111) surfaces considered in DFT calculations; O_2 uptake on annealed Pd/Au(111) surfaces during O_2 King–Wells measurements; AES spectra for as-deposited and annealed 2.9 ML Pd/Au(111) surface; calculated binding energies of O_2 on Pd/Au(111) surfaces; predicted potential energy diagram for O_2 desorption and dissociation on Pd/Au(111) surfaces; O_2 QMS signal during O_2 King–Wells measurement on CO-presaturated Pd/Au(111) surface; calculated binding energies of CO on Pd/Au(111) surfaces; QMS signals during CO-RMBS on oxygen-precovered Pd/Au(111) surfaces at 180 K; calculated enthalpies and initial, transition, and final state configurations for associative and dissociative CO oxidation on Pd/Au(111) surfaces. The Supporting Information is available free of charge on the ACS Publications website at DOI: 10.1021/acs.jpcc.5b02970.

AUTHOR INFORMATION

Corresponding Author

*E-mail: mullins@che.utexas.edu. Phone: 1-512-471-5817.

Notes

The authors declare no competing financial interest.

ACKNOWLEDGMENTS

We are thankful for the generous support of the Department of Energy (DE-FG02-04ER15587 and DE-FG02-13ER16428) and the Welch Foundation (Grants F-1436 for C.B.M. and F-1841 for G.H.). G.M.M. thanks the National Science Foundation for a Graduate Research Fellowship.

REFERENCES

(1) Chen, J. G.; Menning, C. A.; Zellner, M. B. Monolayer Bimetallic Surfaces: Experimental and Theoretical Studies of Trends in Electronic and Chemical Properties. *Surf. Sci. Rep.* **2008**, *63*, 201–254.

(2) Gao, F.; Goodman, D. W. Pd-Au Bimetallic Catalysts: Understanding Alloy Effects from Planar Models and (Supported) Nanoparticles. *Chem. Soc. Rev.* **2012**, *41*, 8009–8020.

(3) Gao, F.; Wang, Y. L.; Goodman, D. W. Reaction Kinetics and Polarization-Modulation Infrared Reflection Absorption Spectroscopy (PM-IRAS) Investigation of CO Oxidation over Supported Pd-Au Alloy Catalysts. *J. Phys. Chem. C* **2010**, *114*, 4036–4043.

(4) Xu, J.; White, T.; Li, P.; He, C. H.; Yu, J. G.; Yuan, W. K.; Han, Y. F. Biphasic Pd-Au Alloy Catalyst for Low-Temperature CO Oxidation. *J. Am. Chem. Soc.* **2010**, *132*, 10398–10406.

(5) Han, Y. F.; Wang, J. H.; Kumar, D.; Yan, Z.; Goodman, D. W. A Kinetic Study of Vinyl Acetate Synthesis over Pd-Based Catalysts: Kinetics of Vinyl Acetate Synthesis over Pd-Au/SiO_2 and Pd/SiO_2 Catalysts. *J. Catal.* **2005**, *232*, 467–475.

(6) Chen, M. S.; Kumar, D.; Yi, C. W.; Goodman, D. W. The Promotional Effect of Gold in Catalysis by Palladium-Gold. *Science* **2005**, *310*, 291–293.

(7) Enache, D. I.; Edwards, J. K.; Landon, P.; Solsona-Espriu, B.; Carley, A. F.; Herzing, A. A.; Watanabe, M.; Kiely, C. J.; Knight, D. W.;

DOI: 10.1021/acs.jpcc.5b02970
J. Phys. Chem. C 2015, 119, 11754–11762

Hutchings, G. J. Solvent-Free Oxidation of Primary Alcohols to Aldehydes Using Au-Pd/TiO_2 Catalysts. *Science* **2006**, *311*, 362−365.
(8) Ketchie, W. C.; Murayama, M.; Davis, R. J. Selective Oxidation of Glycerol over Carbon-Supported AuPd Catalysts. *J. Catal.* **2007**, *250*, 264−273.
(9) Zhang, H. J.; Watanabe, T.; Okumura, M.; Haruta, M.; Toshima, N. Catalytically Highly Active Top Gold Atom on Palladium Nanocluster. *Nat. Mater.* **2012**, *11*, 49−52.
(10) Hutchings, G. J. Nanocrystalline Gold and Gold Palladium Alloy Catalysts for Chemical Synthesis. *Chem. Commun.* **2008**, 1148−1164.
(11) Edwards, J. K.; Solsona, B.; Edwin, N. N.; Carley, A. F.; Herzing, A. A.; Kiely, C. J.; Hutchings, G. J. Switching Off Hydrogen Peroxide Hydrogenation in the Direct Synthesis Process. *Science* **2009**, *323*, 1037−1041.
(12) Campbell, C. T. Bimetallic Surface Chemistry. *Annu. Rev. Phys. Chem.* **1990**, *41*, 775−837.
(13) Somorjai, G. A. Modern Surface Science and Surface Technologies: An Introduction. *Chem. Rev.* **1996**, *96*, 1223−1235.
(14) Weaver, J. F.; Carlsson, A. F.; Madix, R. J. The Adsorption and Reaction of Low Molecular Weight Alkanes on Metallic Single Crystal Surfaces. *Surf. Sci. Rep.* **2003**, *50*, 107−199.
(15) Gong, J. L. Structure and Surface Chemistry of Gold-Based Model Catalysts. *Chem. Rev.* **2012**, *112*, 2987−3054.
(16) Pan, M.; Brush, A. J.; Pozun, Z. D.; Ham, H. C.; Yu, W.-Y.; Henkelman, G.; Hwang, G. S.; Mullins, C. B. Model Studies of Heterogeneous Catalytic Hydrogenation Reactions with Gold. *Chem. Soc. Rev.* **2013**, *42*, 5002−5013.
(17) Conrad, H.; Ertl, G.; Kuppers, J.; Latta, E. E. Interaction of NO and O_2 with Pd(111) surfaces. II. *Surf. Sci.* **1977**, *65*, 245−260.
(18) Matsushima, T. Dissociation of Oxygen Admolecules on Rh(111), Pt(111) and Pd(111) Surfaces at Low Temperatures. *Surf. Sci.* **1985**, *157*, 297−318.
(19) Imbihl, R.; Demuth, J. E. Adsorption of Oxygen on A Pd(111) Surface Studied by High Resolution Electron Energy Loss Spectroscopy (EELS). *Surf. Sci.* **1986**, *173*, 395−410.
(20) Guo, X. C.; Hoffman, A.; Yates, J. T. Adsorption Kinetics and Isotopic Equilibration of Oxygen Adsorbed on the Pd(111) Surface. *J. Chem. Phys.* **1989**, *90*, 5787−5792.
(21) Kolasinski, K. W.; Cemic, F.; Hasselbrink, E. O_2/Pd(111) - Clarification of the Correspondence between Thermal-Desorption Features and Chemisorption States. *Chem. Phys. Lett.* **1994**, *219*, 113−117.
(22) Rose, M. K.; Borg, A.; Dunphy, J. C.; Mitsui, T.; Ogletree, D. F.; Salmeron, M. Chemisorption and Dissociation of O_2 on Pd(111) Studied by STM. *Surf. Sci.* **2003**, *547*, 162−170.
(23) Nolan, P. D.; Lutz, B. R.; Tanaka, P. L.; Mullins, C. B. Direct Verification of A High-Translational-Energy Molecular Precursor to Oxygen Dissociation on Pd(111). *Surf. Sci.* **1998**, *419*, L107−L113.
(24) Min, B. K.; Friend, C. M. Heterogeneous Gold-Based Catalysis for Green Chemistry: Low-Temperature CO Oxidation and Propene Oxidation. *Chem. Rev.* **2007**, *107*, 2709−2724.
(25) Li, Z. J.; Gao, F.; Tysoe, W. T. Carbon Monoxide Oxidation over Au/Pd(100) Model Alloy Catalysts. *J. Phys. Chem. C* **2010**, *114*, 16909−16916.
(26) Gao, F.; Wang, Y. L.; Goodman, D. W. CO Oxidation over AuPd(100) from Ultrahigh Vacuum to Near-Atmospheric Pressures: The Critical Role of Contiguous Pd Atoms. *J. Am. Chem. Soc.* **2009**, *131*, 5734−5735.
(27) Piednoir, A.; Languille, M. A.; Piccolo, L.; Valcarcel, A.; Aires, F.; Bertolini, J. C. Pd(111) versus Pd-Au(111) in Carbon Monoxide Oxidation under Elevated Pressures. *Catal. Lett.* **2007**, *114*, 110−114.
(28) Zhang, J.; Jin, H. M.; Sullivan, M. B.; Chiang, F.; Lim, H.; Wu, P. Study of Pd-Au Bimetallic Catalysts for CO Oxidation Reaction by DFT Calculations. *Phys. Chem. Chem. Phys.* **2009**, *11*, 1441−1446.
(29) Ham, H. C.; Hwang, G. S.; Han, J.; Nam, S. W.; Lim, T. H. On the Role of Pd Ensembles in Selective H_2O_2 Formation on PdAu Alloys. *J. Phys. Chem. C* **2009**, *113*, 12943−12945.
(30) Ham, H. C.; Hwang, G. S.; Han, J.; Nam, S. W.; Lim, T. H. Geometric Parameter Effects on Ensemble Contributions to Catalysis: H_2O_2 Formation from H_2 and O_2 on AuPd Alloys. A First Principles Study. *J. Phys. Chem. C* **2010**, *114*, 14922−14928.
(31) Ham, H. C.; Stephens, J. A.; Hwang, G. S.; Han, J.; Nam, S. W.; Lim, T. H. Pd Ensemble Effects on Oxygen Hydrogenation in AuPd Alloys: A Combined Density Functional Theory and Monte Carlo Study. *Catal. Today* **2011**, *165*, 138−144.
(32) Ham, H. C.; Stephens, J. A.; Hwang, G. S.; Han, J.; Nam, S. W.; Lim, T. H. Role of Small Pd Ensembles in Boosting CO Oxidation in AuPd Alloys. *J. Phys. Chem. Lett.* **2012**, *3*, 566−570.
(33) Garcia-Mota, M.; Lopez, N. The Role of Long-Lived Oxygen Precursors on AuM Alloys (M = Ni, Pd, Pt) in CO Oxidation. *Phys. Chem. Chem. Phys.* **2011**, *13*, 5790−5797.
(34) Wang, T. Y.; Li, B. H.; Yang, J. H.; Chen, H.; Chen, L. A. First Principles Study of Oxygen Adsorption and Dissociation on the Pd/Au Surface Alloys. *Phys. Chem. Chem. Phys.* **2011**, *13*, 7081−7089.
(35) Yuan, D. W.; Liu, Z. R.; Chen, J. H. Catalytic Activity of Pd Ensembles over Au(111) Surface for CO Oxidation: A First-Principles Study. *J. Chem. Phys.* **2011**, *134*, 054704.
(36) Yuan, D. W.; Liu, Z. R.; Xu, S. First-Principles Investigations of O_2 Dissociation on Low-Coordinated Pd Ensembles over Stepped Au Surfaces. *Phys. Lett. A* **2012**, *376*, 3432−3438.
(37) Yuan, D. W.; Liu, Z. R. Catalytic Activity of Pd Ensembles Incorporated into Au Nanocluster for CO oxidation: A First-Principles Study. *Phys. Lett. A* **2011**, *375*, 2405−2410.
(38) Kim, H. Y.; Henkelman, G. CO Adsorption-Driven Surface Segregation of Pd on Au/Pd Bimetallic Surfaces: Role of Defects and Effect on CO Oxidation. *ACS Catal.* **2013**, *3*, 2541−2546.
(39) Cheng, D. J.; Xu, H. X.; Fortunelli, A. Tuning the Catalytic Activity of Au-Pd Nanoalloys in CO Oxidation via Composition. *J. Catal.* **2014**, *314*, 47−55.
(40) Flaherty, D. W.; Hahn, N. T.; Ferrer, D.; Engstrom, T. R.; Tanaka, P. L.; Mullins, C. B. Growth and Characterization of High Surface Area Titanium Carbide. *J. Phys. Chem. C* **2009**, *113*, 12742−12752.
(41) Flaherty, D. W.; Yu, W.-Y.; Pozun, Z. D.; Henkelman, G.; Mullins, C. B. Mechanism for the Water-Gas Shift Reaction on Monofunctional Platinum and Cause of Catalyst Deactivation. *J. Catal.* **2011**, *282*, 278−288.
(42) Yu, W.-Y.; Mullen, G. M.; Mullins, C. B. Hydrogen Adsorption and Absorption with Pd-Au Bimetallic Surfaces. *J. Phys. Chem. C* **2013**, *117*, 19535−19543.
(43) Yu, W.-Y.; Mullen, G. M.; Mullins, C. B. Interactions of Hydrogen and Carbon Monoxide on Pd-Au Bimetallic Surfaces. *J. Phys. Chem. C* **2014**, *118*, 2129−2137.
(44) Yu, W.-Y.; Mullen, G. M.; Flaherty, D. W.; Mullins, C. B. Selective Hydrogen Production from Formic Acid Decomposition on Pd-Au Bimetallic Surfaces. *J. Am. Chem. Soc.* **2014**, *136*, 11070−11078.
(45) Koel, B. E.; Sellidj, A.; Paffett, M. T. Ultrathin Films of Pd on Au(111) - Evidence for Surface Alloy Formation. *Phys. Rev. B* **1992**, *46*, 7846−7856.
(46) King, D. A.; Wells, M. G. Reaction Mechanism in Chemisorption Kinetics - Nitrogen on {100} Plane of Tungsten. *Proc. R. Soc. London, Ser. A* **1974**, *339*, 245−269.
(47) Wheeler, M. C.; Seets, D. C.; Mullins, C. B. Kinetics and Dynamics of the Initial Dissociative Chemisorption of Oxygen on Ru(001). *J. Chem. Phys.* **1996**, *105*, 1572−1583.
(48) Davis, J. E.; Karseboom, S. G.; Nolan, P. D.; Mullins, C. B. Kinetics and Dynamics of the Initial Adsorption of Nitric Oxide on Ir(111). *J. Chem. Phys.* **1996**, *105*, 8362−8375.
(49) Davis, J. E.; Nolan, P. D.; Karseboom, S. G.; Mullins, C. B. Kinetics and Dynamics of the Dissociative Chemisorption of Oxygen on Ir(111). *J. Chem. Phys.* **1997**, *107*, 943−952.
(50) Kresse, G.; Hafner, J. Ab Initio Molecular Dynamics for Liquid Metals. *Phys. Rev. B* **1993**, *47*, 558−561.
(51) Kresse, G.; Hafner, J. Ab Initio Molecular-Dynamics Simulation of the Liquid-Metal−Amorphous-Semiconductor Transition in Germanium. *Phys. Rev. B* **1994**, *49*, 14251−14269.

DOI: 10.1021/acs.jpcc.5b02970
J. Phys. Chem. C 2015, 119, 11754−11762

(52) Kresse, G.; Furthmuller, J. Efficient Iterative Schemes for Ab Initio Total-Energy Calculations Using A Plane-Wave Basis Set. *Phys. Rev. B* **1996**, *54*, 11169−11186.
(53) Kresse, G.; Furthmuller, J. Efficiency of Ab-Initio Total Energy Calculations for Metals and Semiconductors Using A Plane-Wave Basis Set. *Comput. Mater. Sci.* **1996**, *6*, 15−50.
(54) Blochl, P. E. Projector Augmented-Wave Method. *Phys. Rev. B* **1994**, *50*, 17953−17979.
(55) Hohenberg, P.; Kohn, W. Inhomogeneous Electron Gas. *Phys. Rev. B* **1964**, *136*, B864−B871.
(56) Kohn, W.; Sham, L. J. Self-Consistent Equations Including Exchange and Correlation Effects. *Phys. Rev.* **1965**, *140*, 1133−1138.
(57) Perdew, J. P.; Burke, K.; Ernzerhof, M. Generalized Gradient Approximation Made Simple. *Phys. Rev. Lett.* **1996**, *77*, 3865−3868.
(58) Henkelman, G.; Uberuaga, B. P.; Jonsson, H.; Climbing Image, A. Nudged Elastic Band Method for Finding Saddle Points and Minimum Energy Paths. *J. Chem. Phys.* **2000**, *113*, 9901−9904.
(59) Henkelman, G.; Jonsson, H. Improved Tangent Estimate in the Nudged Elastic Band Method for Finding Minimum Energy Paths and Saddle Points. *J. Chem. Phys.* **2000**, *113*, 9978−9985.
(60) Monkhorst, H. J.; Pack, J. D. Special Points for Brillouin-Zone Integrations. *Phys. Rev. B* **1976**, *13*, 5188−5192.
(61) Yi, C. W.; Luo, K.; Wei, T.; Goodman, D. W. The Composition and Structure of Pd-Au Surfaces. *J. Phys. Chem. B* **2005**, *109*, 18535−18540.
(62) Wei, T.; Wang, J.; Goodman, D. W. Characterization and Chemical Properties of Pd-Au Alloy Surfaces. *J. Phys. Chem. C* **2007**, *111*, 8781−8788.
(63) Li, Z.; Gao, F.; Wang, Y.; Calaza, F.; Burkholder, L.; Tysoe, W. T. Formation and characterization of Au/Pd surface alloys on Pd(111). *Surf. Sci.* **2007**, *601*, 1898−1908.
(64) Trenary, M. Reflection Absorption Infrared Spectroscopy and the Structure of Molecular Adsorbates on Metal Surfaces. *Annu. Rev. Phys. Chem.* **2000**, *51*, 381−403.
(65) Meier, D. C.; Bukhtiyarov, V.; Goodman, D. W. CO Adsorption on Au(110)-(1 × 2): An IRAS Investigation. *J. Phys. Chem. B* **2003**, *107*, 12668−12671.
(66) Campbell, C. T.; Arnadottir, L.; Sellers, J. R. V. Kinetic Prefactors of Reactions on Solid Surfaces. *Z. Phys. Chem.* **2013**, *227*, 1435−1454.
(67) Kolasinski, K. W.; Cemic, F.; Demeijere, A.; Hasselbrink, E. Interactions in Co-Adsorbed CO+O_2/Pd(111) Layers. *Surf. Sci.* **1995**, *334*, 19−28.
(68) Engel, T.; Ertl, G. Surface Residence Times and Reaction Mechanism in Catalytic Oxidation of CO on Pd(111). *Chem. Phys. Lett.* **1978**, *54*, 95−98.
(69) Conrad, H.; Ertl, G.; Kuppers, J. Interactions between Oxygen and Carbon Monoxide on A Pd(111) Surface. *Surf. Sci.* **1978**, *76*, 323−342.
(70) Engel, T.; Ertl, G. A Molecular Beam Investigation of Catalytic Oxidation of CO on Pd(111). *J. Chem. Phys.* **1978**, *69*, 1267−1281.
(71) Libuda, J.; Freund, H. J. Molecular Beam Experiments on Model Catalysts. *Surf. Sci. Rep.* **2005**, *57*, 157−298.

DOI: 10.1021/acs.jpcc.5b02970
J. Phys. Chem. C 2015, 119, 11754−11762